9

INJURY BIOMECHANICS RESEARCH
Proceedings of the Thirtieth International Workshop

Development of Finite Element Human Neck Model for the SIMON Program

H.Y. Choi, I.H. Lee, E. Haug, E. Takhounts, and R. Eppinger

ABSTRACT

A finite element model development of a 50th percentile male cervical spine is presented in this paper. The model consists of rigid, geometrically accurate vertebrae held together with deformable intervertibral disks, facet joints, and ligaments modeled as a series of nonlinear springs. These deformable structures were rigorously tuned, through failure, to mimic existing experimental data; first as functional unit characterizations at three cervical levels and then as a fully assembled c-spine using the experimental data from Duke University and other data in the NHTSA database. The validated model is intended for use as a post processor of dummy measurement within the simulated injury monitor (SIMon) concept being developed by NHTSA where measured kinematics and kinetic data obtained from a dummy during a crash test will serve as the boundary conditions to "drive" the finite element model of the neck. The post-processor will then interrogate the model to determine whether any ligament have exceeded its known failure limit. The detailed information of structures and validation process of the anatomical human neck model used for the SIMon program will be presented.

INTRODUCTION

For the crash injury assessment of vehicle occupants, anthropometric test devices such as crash dummies are commonly employed both in experimental and numerical studies. Displacements, accelerations and forces measured on crash dummy constitute injury criteria which statistically quantify the potential degrees of injuries. Recently, the modeling of humans in the numerical crash simulation is widely in progress in parallel with the attempts of design enhancement of current crash dummies for the better biofidelity and measuring capabilities. Numerical try-out with human models in the crash simulation is somewhat favorable since it can provide the basic injury mechanisms and also can predict real crash injuries such as bone fractures and ligament ruptures. However, the injury assessment using numerical human model has not yet obtained general legitimate approvals. The concept of simulated injury monitor, SIMon originally proposed by NHTSA, fills the gap between two different applications in injury assessment using crash dummies and numerical human models. Crash dummy measurements, such as neck loads and kinematics of head and torso, are the external input conditions for the calculation of responses of the anatomical human neck model in the SIMon neck program. Thus, the SIMon

neck program consists of PC Window based finite element solver, anatomic human neck model, and the graphic interface. In this paper, the detailed information of structures and validation process of the anatomical human neck model used for the SIMon program will be presented. Newly proposed neck injury criteria from this study, based on the degrees of ligament and disc ruptures, will be analyzed in comparison with N_{ij} neck injury criteria.

FINITE ELEMENT MODELING OF HUMAN NECK

The model, anatomically depicted in detail, was built on 50% male geometry. The hard and soft tissues in the neck such as vertebrae, muscles, ligaments, organs, discs and fatty tissues were modeled by using the various kinds of finite elements and material properties to represent adequate mechanical behaviors of each component. Figure 1 shows the SIMon neck model developed in this study.

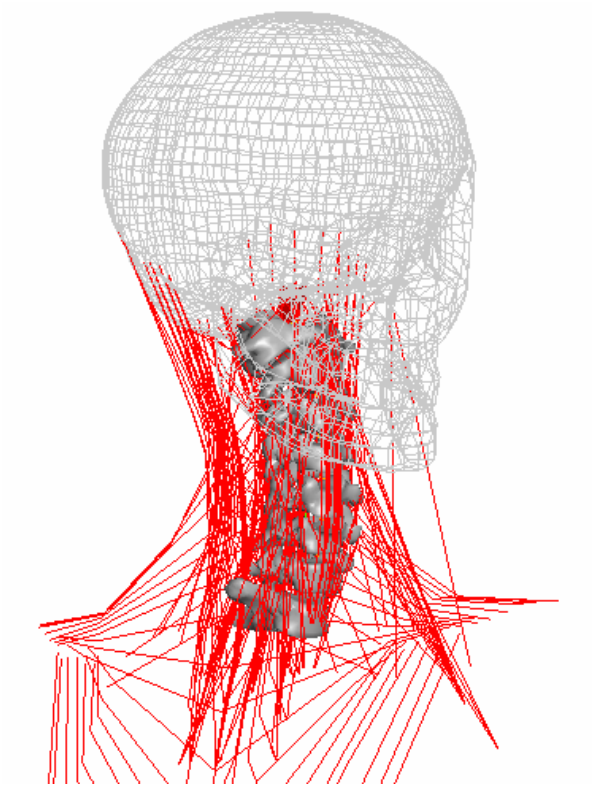

Figure 1: Finite element human neck model for SIMon program

Cervical Vertebrae

The geometry of vertebrae was adopted from Viewpoint Datalab™ (VP2488: Points-11025, polygons-15726, www.viewpoint.com). Figure 2 is the corresponding 3-D CAD drawing in IGES format. From Figures. 3 to 5, selected finite element models of cervical vertebrae are shown with corresponding anatomical features. Since the each vertebra bone was modeled as a rigid body, geometrical inertia characteristics such as center of gravity, mass moment of inertia and mass are required. These kinematic properties (Table 1) were calculated based on the cross sectional geometries and different densities of bony external (cortical bone) and internal (trabecular bone) structure of cervical vertebrae.

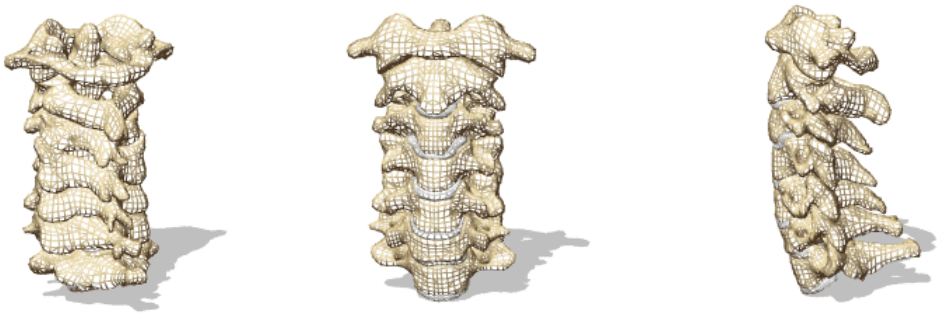

(a) posterior view (b) front view (c) lateral view

Figure 2: Three-dimensional CAD drawing in IGES format [2]

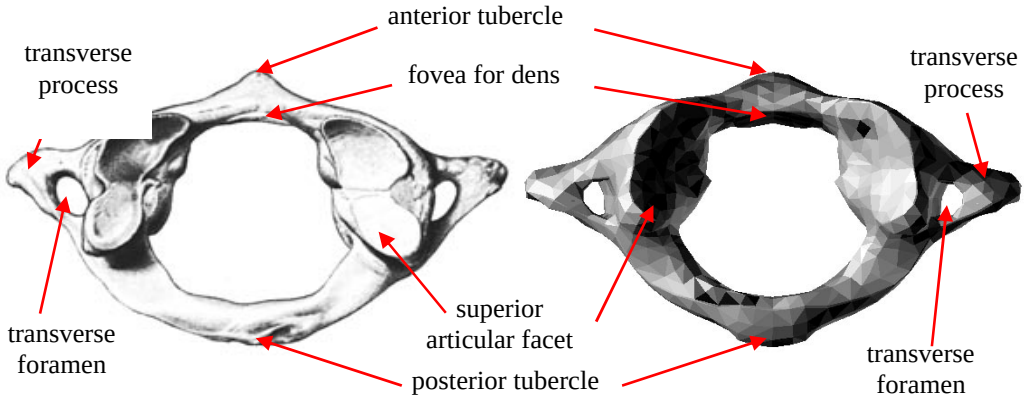

(a) anatomy (Gray, 1918) (b) SIMON neck

Figure 3: Atlas (C1)

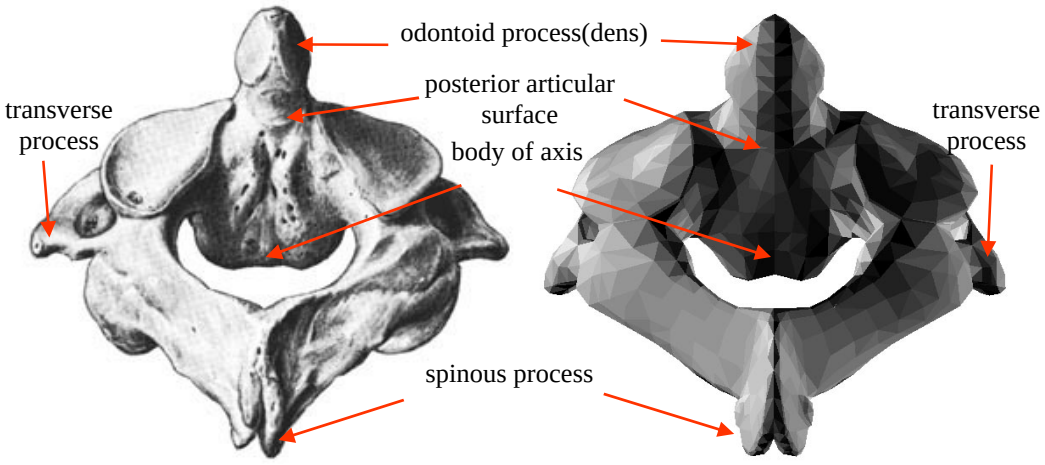

(a) anatomy (Gray, 1918) (b) SIMON neck

Figure 4: Axis (C2)

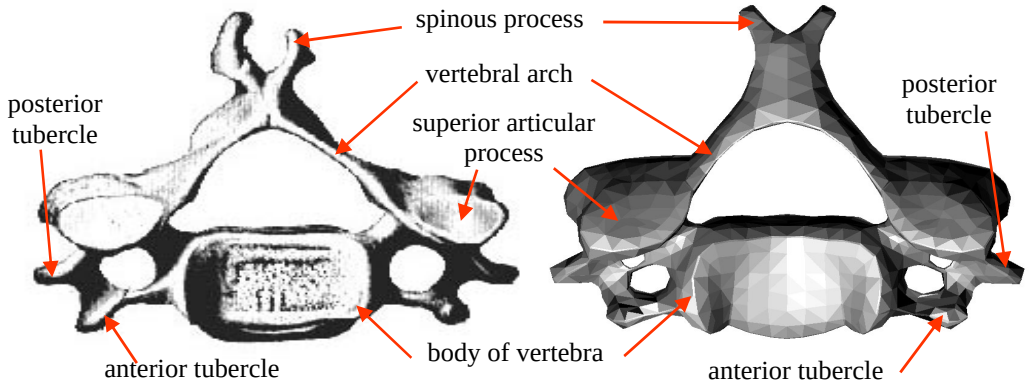

(a) anatomy (Gray, 1918) (b) SIMON neck

Figure 5: 5th cervical vertebra (C5)

Table 1. Mass And Inertia Properties Of Cervical Vertebrae In The SIMON Neck

Vertebra	Mass (g)	Inertia (kg/mm^2)		
		I_{rr}	I_{ss}	I_{tt}
C1	19.43	7.797	2.804	9.770
C2	21.35	5.921	3.921	3.897
C3	13.88	2.268	1.656	3.416
C4	14.83	3.020	1.744	4.063
C5	16.34	3.289	1.958	4.508
C6	16.69	3.383	2.693	5.366
C7	16.38	2.886	2.584	4.797

(r, s, t represent the principal axes, front, lateral and superior directions, respectively)

Intervertebral Discs

Each disc is composed of nucleus pulposus, annulus fibrous, and cartilageous end-plate. Between 70 to 90 % of the nucleus pulposus by weight is water, and takes up as much as 40 to 60 % of the disc area. The annulus fibrous is a laminated and hence anisotropic structure composed of several layers in which each layers maintain a 30 degree angle of inclination from the horizontal plane. The inner boundary of the annulus fibrous is attached to cartilageous end-plate, and the outer surface is directly connected to vertebra body. The discs play dominant role in sustaining the body against compressive load. The discs show greater stiffness for the front/rearward motions than for the side/side motion, with the annulus fibrous rather the nucleus pulposus making a major contribution. In SIMon neck model, complex deformation of the discs was modeled by using 6-DOF kinematic joint element. For defining the kinematic joint elements, three translational force-deflection and three rotational moment-angle relations are needed. Basic information for these relationships was adopted from reported experimental measurements (Pintar, 1986, Yoganandan, et al, 2001, Moroney, 1998). Figure 6 shows the mechanical properties applied to 6 DOF kinematic joint element of disc between C4 and C5.

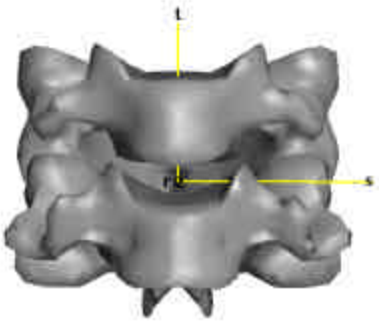

frontal view

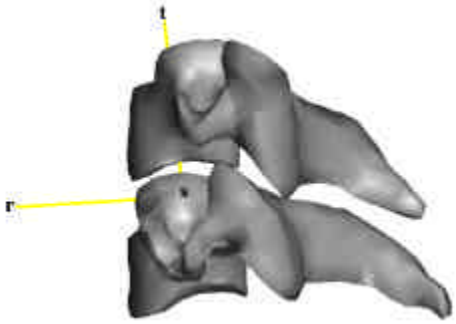

lateral view

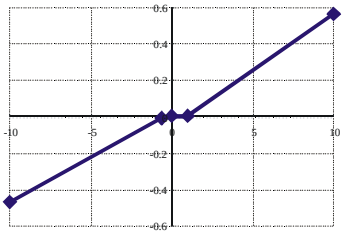

Fore/aft (kN-mm)

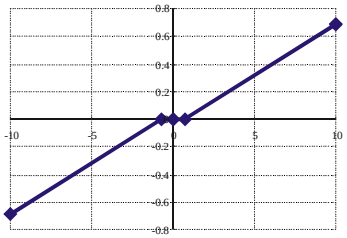

Medial/lateral (kN-mm)

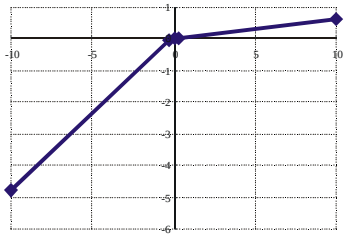

Tension/compression (kN-mm)

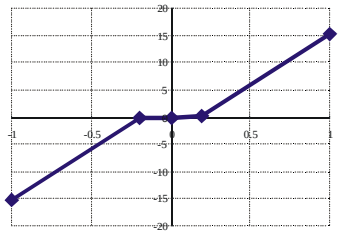

Lateral bending (Nm-radian)

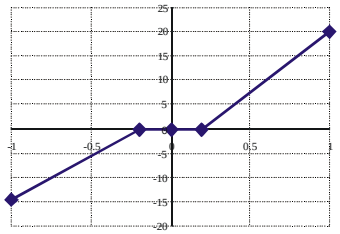

Flexion/extension (Nm-radian)

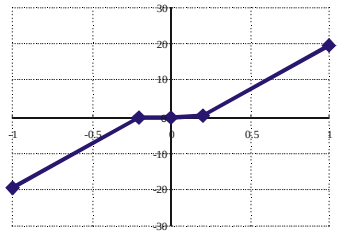

Torsion (Nm-radian)

Figure 6: DOF mechanical properties of disc between C4 and C5

Ligarments

A ligament is one of the two connecting tissues for the human cervical spine. Its function is to ensure that the spinal motion occurs within some physiological bound, thus preventing spinal code injury due to excessive spinal motion. The ligament is usually situated between the two adjacent vertebrae, and in some cases, even connects several vertebrae. While the ligament shows high strength against tension along the axial direction, it cannot support much compressive load. To account for the visco-elastic and anisotropic biomechanical properties of the ligament, nonlinear one dimensional bar element that can support only tensile load was used for the numerical simulation purpose. For cruciform, transverse, and tectorial ligaments in atlanto-axial joint however, membrane elements were used instead to allow for surface contact. Figures 7 through 11 show selected finite element models of ligaments with corresponding anatomical features.

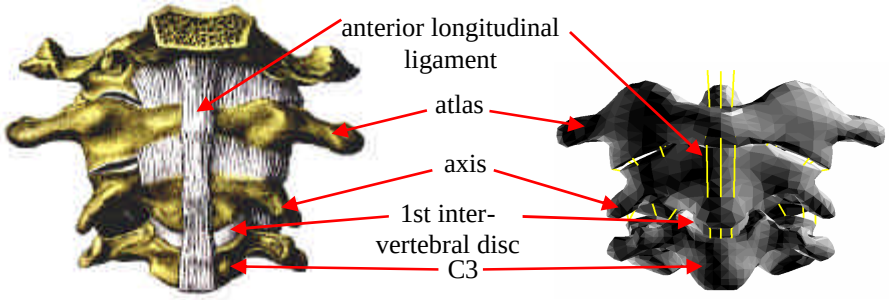

(a) anatomy (Gray, 1918) (b) SIMON neck

Figure 7: Articulations of occipital bone and C1~C3 (front view)

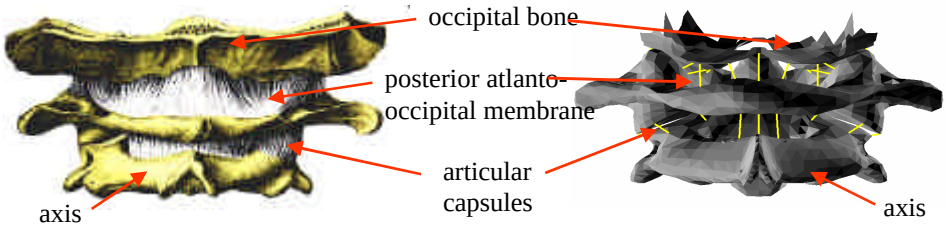

(a) anatomy (Gray, 1918) (b) SIMON neck

Figure 8: Occipital-atlanto-axial joints (posterior view)

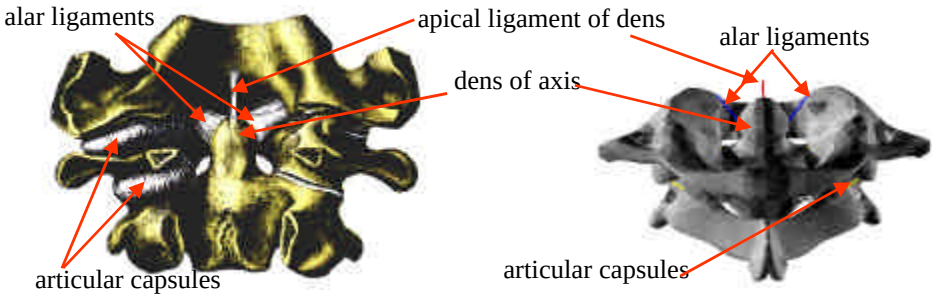

(a) anatomy (Gray, 1918) (b) SIMON neck

Figure 9: Alar and apical ligaments (posterior view)

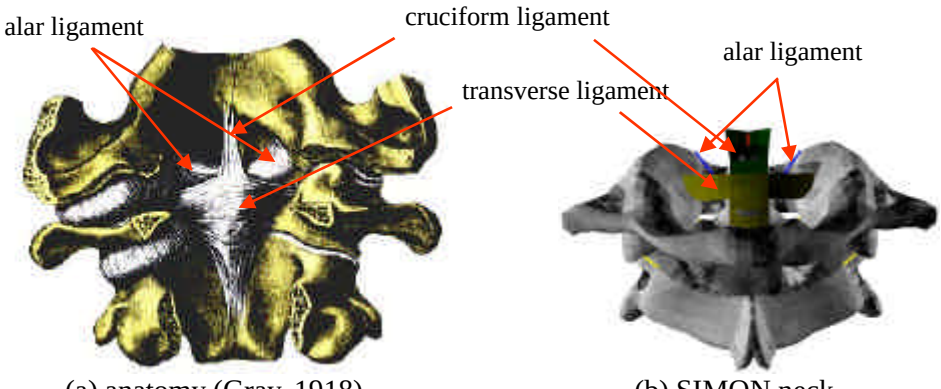

(a) anatomy (Gray, 1918) (b) SIMON neck

Figure 10: Atlanto-axial joints (posterior view)

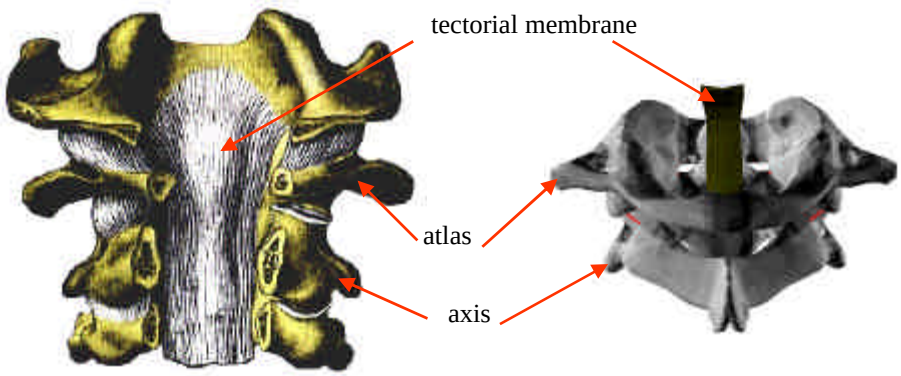

(a) anatomy (Gray, 1918) (b) SIMON neck

Figure 11: Median section of atlanto-axial joints

A typical behavior of the ligament under tensile load is shown in Figure 12 (Yoganandan, 2001). OA denotes the ambient phase or toe region representing a highly non-linear curve corresponding to low stiffness; AB denotes the most linear phase (these two correspond to physiologic loading); BC denotes the traumatic phase (region of gradually decreasing stiffness); C denotes failure. Post-traumatic phase is represented by the portion of the curve beyond the traumatic phase (arrow). OA^1, A^1B^1, B^1C^1 denote the stiffness pattern in these phases. At the point of failure, the stiffness is zero. The physiologic, traumatic, and post-traumatic phases were renamed as neutral, elastic, and plastic zones, respectively.

As shown in Figures 7 through 11, each ligament was modeled by parallel connections of multiple single-bar elements. Thus, the reactive force existing in each ligament is a sum of forces developed by individual elements constituting that ligament. The damping effect in the ligament was modeled by viscoelastic characteristics (Nitsche, 1996) shown in Figure 13

Figure 14 shows the force-deformation curves of C2/C3 ligaments applied in SIMon neck model. Each curve has bi-linear regions which represent the neutral and elastic stiffnesses. The stiffness values are based on the segmental test results (Pintar, 1986, Yoganandan, et al, 2001, de Jagor, 1996).

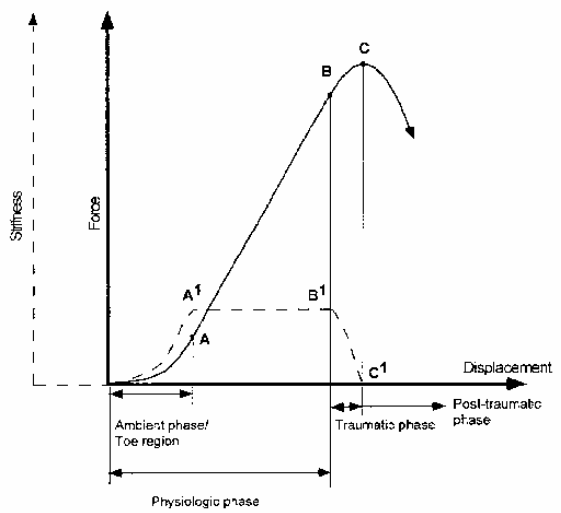

Figure 12: Schematic drawing of tensile behavior of ligament (Yoganandan, 2001)

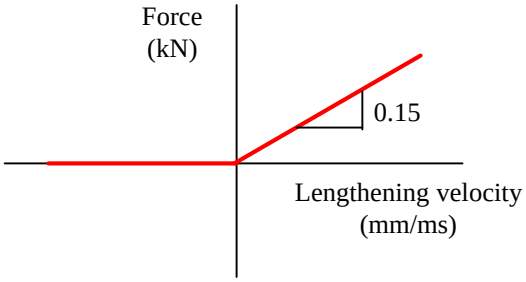

Figure 13: Damping factors for cervical ligaments

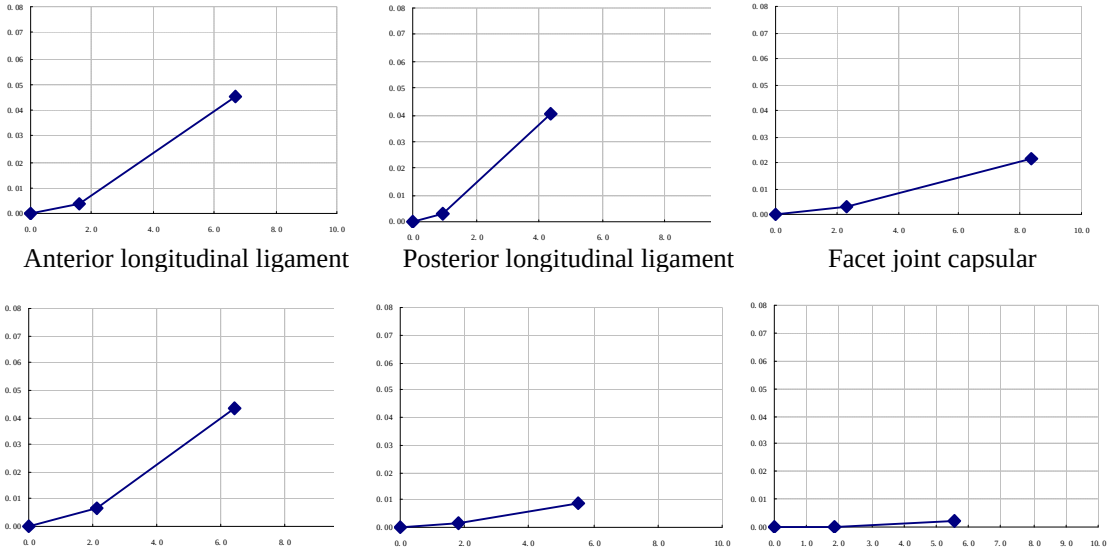

Anterior longitudinal ligament | Posterior longitudinal ligament | Facet joint capsular

Ligament flava | Inter-Spinous Ligament | Inter-Transverse Ligament

Figure 14: Force-deformation curves of C2/C3 ligaments

Muscles

Twenty two pairs of cervical muscles listed in Table 2 were included in the model. One dimensional bar elements were used for each muscle segment (Figure 15). Depending on its anatomical shape, single element or multiple elements serially joined were attached at the origin and insertion points of relevant skeletons. Hill's muscle model was utilized to generate both active and passive muscle forces. The muscle activation level was assumed to be the same for all modeled muscles and the degree of activation was set to correctly predict available human volunteer experimental data from NBDL and JARI.

Table 2. List of cervical muscles in SIMon neck model

Locations	Muscles
Anterior (flexors)	Longus colli, Longus capitis, Scalenus anterior, Scalenus medius, Scalnus posterior, Sternocleidomastoid
Posterior (extensors)	Splenius capitis, Splenius cervicis, Semispinalis capitis, Semispinalis cervicis, Longissimus capitis, Longissimus cervicis, Multifidus cervicis, Levator scapulae , Rectus capitis anterior,

	Rectus capitis lateralis, Rectus capitis posterior major, Rectus capitis posterior minor, Obliquus capitis superior, Obliquus capitis inferior, Trapezius, Rotatores

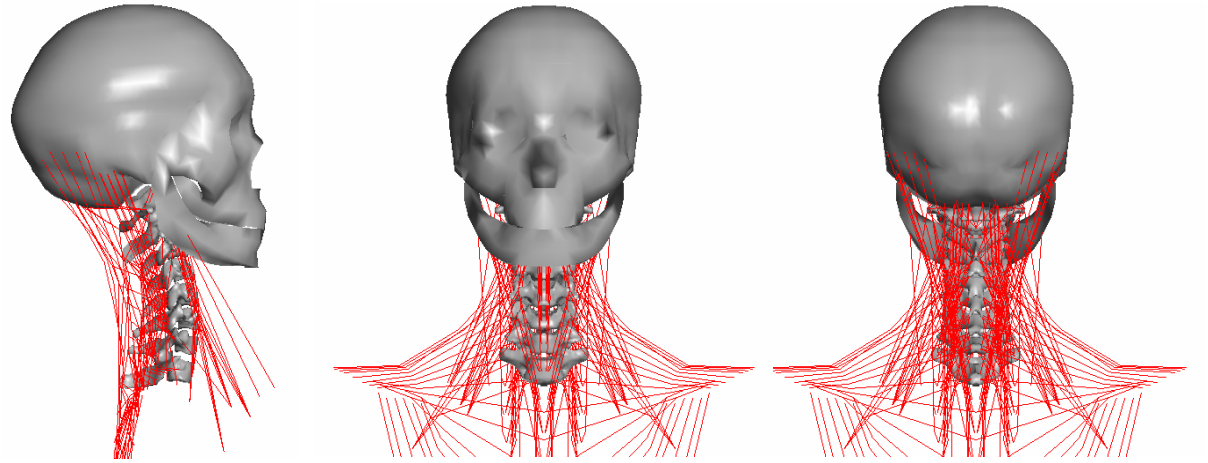

Figure 15: Muscles in SIMon neck model

VALIDATIONS

The SIMon neck model has been validated against available experimental data. The functional motion units at three cervical levels were chosen for both bending and tensile behaviors. Then, fully assembled c-spine under the tensile loading was simulated for the validation of overall compliance of the cervical spine.

Tensile and bending responses for functional cervical spine units

For validation of tensile stiffness and failure load of SIMon neck model, test results of unembalmed human cadaver performed by Duke University (Myers, 2002) were used. In the Duke test, three functional motion units (FMU), OC/C2, C4/C5 and C6/C7 were placed in a testing device designed to apply pure vertical loads. Figure 16 shows the loading and boundary conditions in the simulation which are equivalent to the test condition.

As we can see from Figure 17, simulation result with SIMon neck model correlates well with the test results. The similar correlations were obtained from other two FMU simulations.

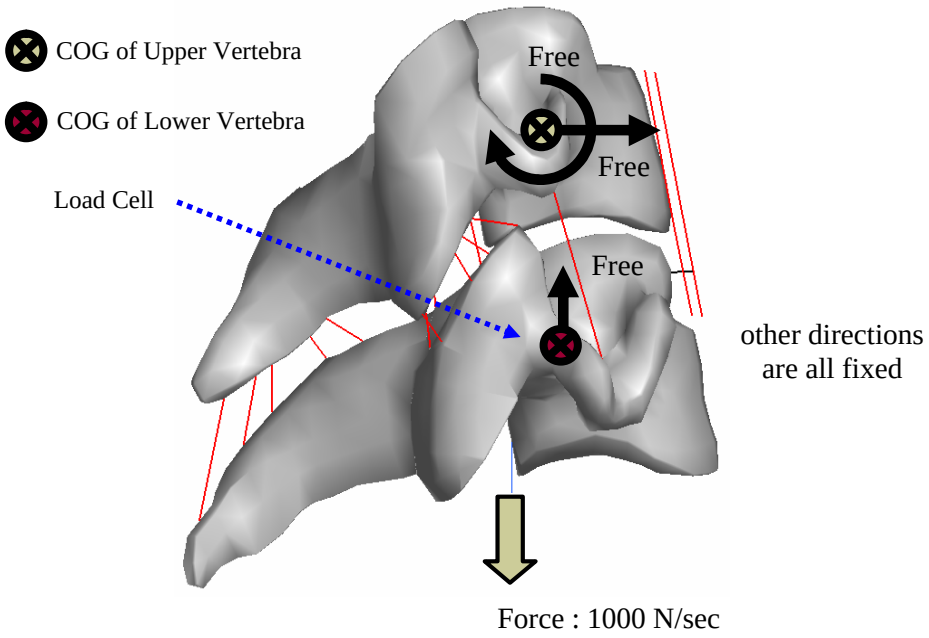

Figure 16: Tensile loading and boundary conditions for FMU simulation

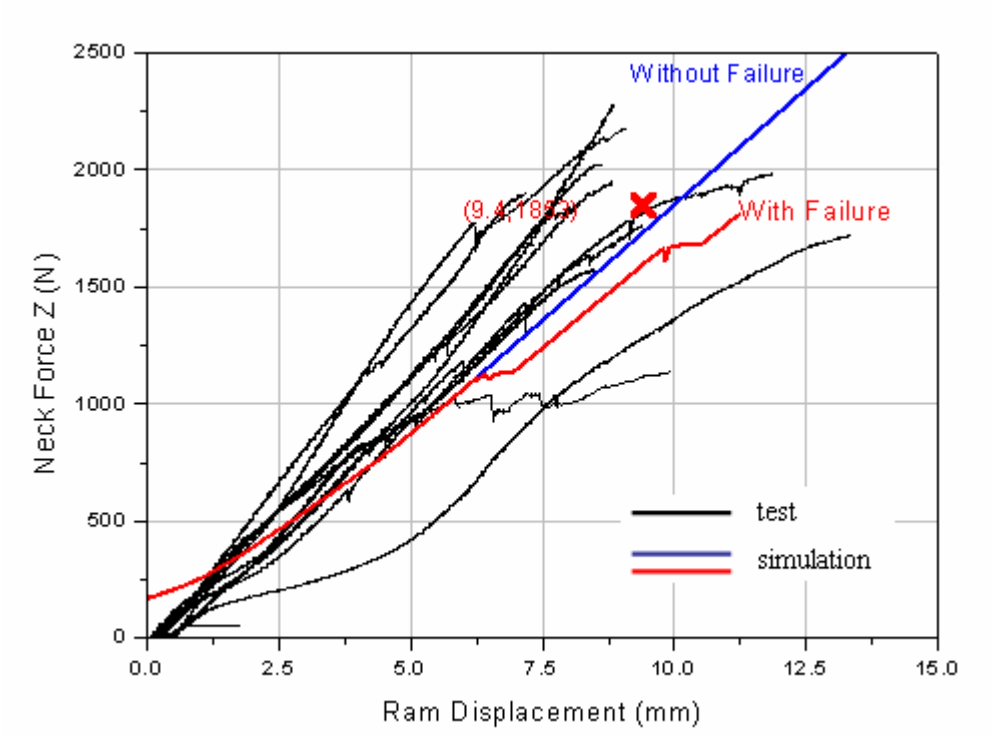

Figure 17: Comparison of tensile force-deflection at C4/C5 FMU between test and simulation

Compliance test of extension and flexion performed by Duke University in series with above mentioned tension test was utilized to verify bending characteristics of the model. In the Duke test, three functional motion units, OC/C2, C5/C6 and C7/T1 were placed in a testing device designed to apply pure bending moment. Figure 18 shows the loading and boundary conditions in the simulation which are equivalent to the test condition.

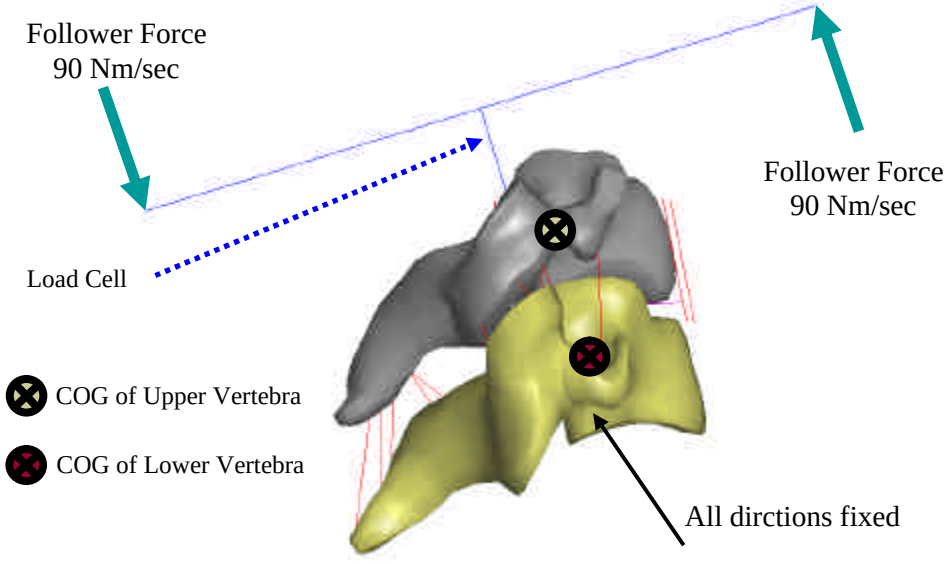

Figure 18 Bending and boundary conditions for FMU simulation

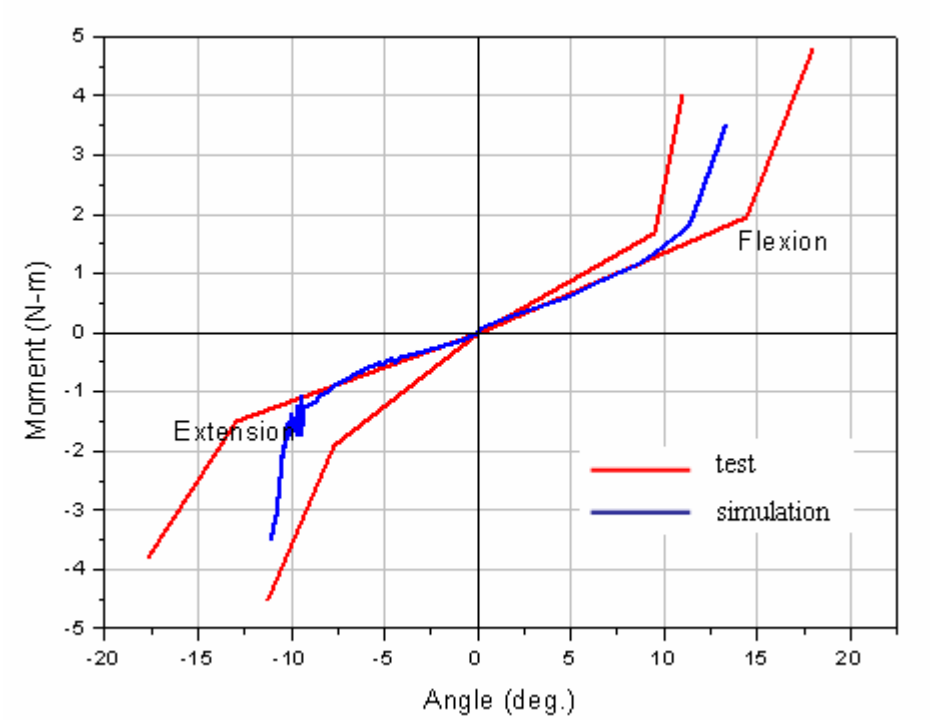

Figure 19: Comparison of bending moment-angle at C5/C6 FMU between test and simulation

As we can see from Figure 19, simulation result with SIMon neck model correlates well with the test results. The similar correlations were obtained from other two FMU simulations.

Tensile responses for whole cervical spine

The tensile compliance of whole cervical spine was simulated with two kinds of end conditions. Figure 20 shows the loading and boundary conditions in the simulation which are equivalent to the test condition.

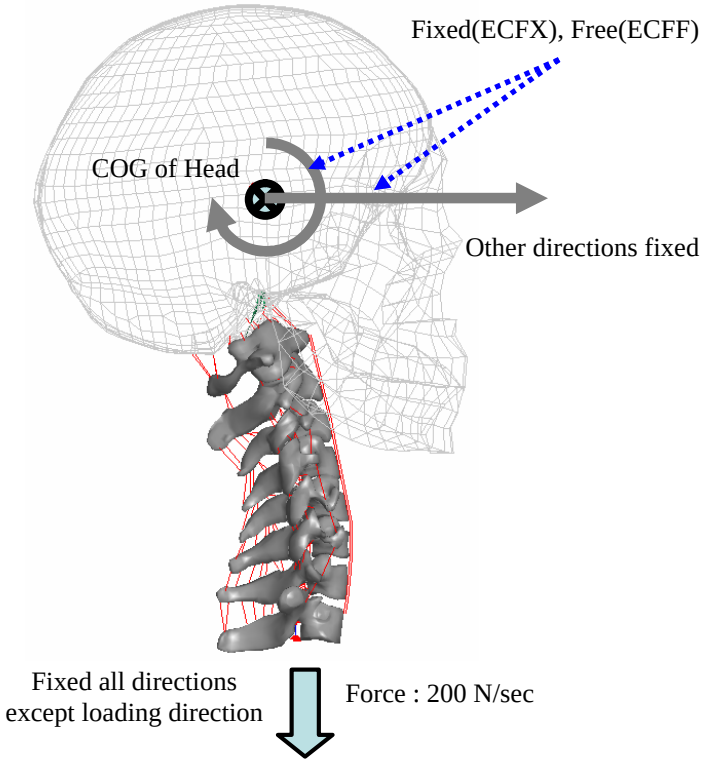

Figure 20: Loading and boundary conditions for WCS simulation

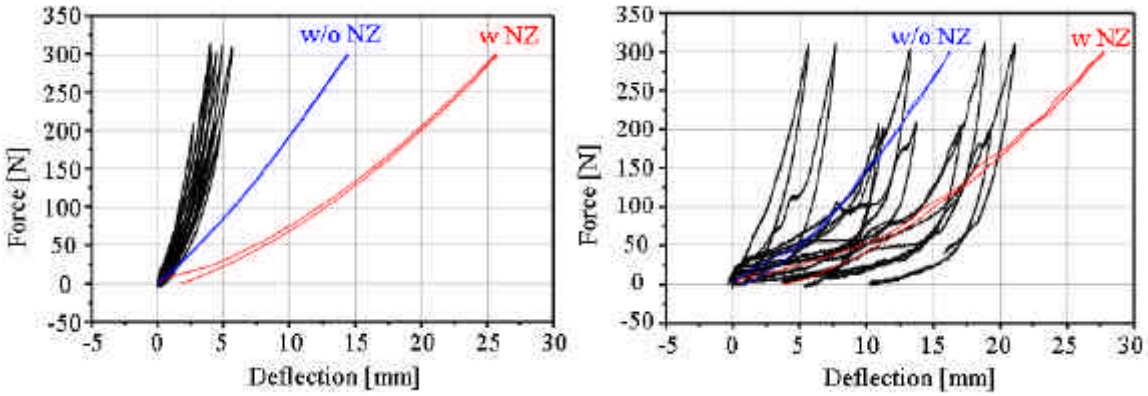

(a) Fixed-Fixed end condition (b) Fixed-Free end condition

Figure 21: Comparison of force-deflection relationship of WCS between test and simulation

As shown in Figure 21, the global stiffness of whole cervical spine of SIMon neck model shows considerably smaller values in both end conditions in comparison with Duke test measurements.

CONCLUSIONS

The poor correlations of SIMon neck model for whole cervical spine tensile characteristics are mainly due to the effects of extra compliance and frictions at fixation and frames in test. By accounting for those effects which was quantified by Duke University (Nightingale, 2003) in the model, the prediction for the compliance of WCB becomes substantially improved as shown in Figure 22. The details of model reformation to take those extra compliance and frictions into account will be introduced at the next workshop.

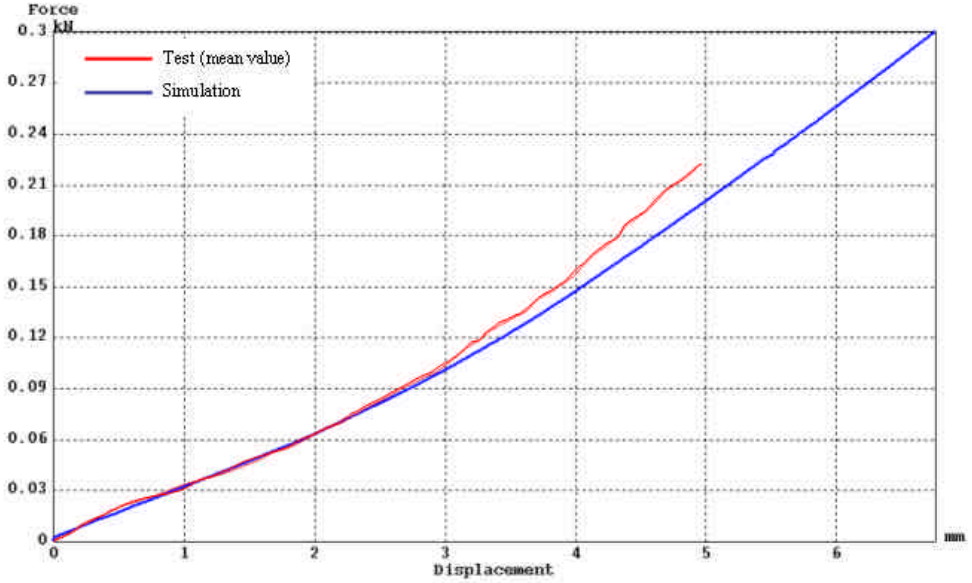

Figure 22: Comparison of force-deflection relationship of WCS between test and simulation (recalculated for Fixed-Fixed case with updated model)

ACKNOWLEDGEMENTS

This study was supported, in part, by Korean ministry of science and technology. (Project No.: M10139080001-02B0808-00210)

REFERENCES

DE JAGER, MARKO (1996) Mathematical Head-Neck Models for Acceleration Impacts, Ph.D. thesis, University of Technology,

GRAY, H. (1918) Anatomy of the human body, Lea & Febiger,

NITSCHE, S., HAUG, E. and KISIELEWICZ, L. T. (1996) Validation of a Finite Element Model of the Human Neck, ESI Group

MORONEY, S. P., SCHULTZ, A. B., MILLER, J. A. A., ANDERSSON, G. B. J. (1998) Load- displacement properties of lower cervical spine motion segments, Journal of Biomechanics, Vol. 21, No. 9, pp. 769~779

MYERS, B. (2002) personal communication

NIGHTINGLALE, R. (2003) personal communication

PINTER, F. A. (1986) The biomechanics of spinal elements, Ph.D Thesis, Marquette University,

YOGANANDAN, N., KUMARESAN, S., PINTAR, F. A. (2001) Biomechanics of the cervical spine Part 2. Cervical spine soft tissue responses and biomechanical modeling, Clinical Biomechanics Vol. 16, pp1~27